Pergamon

SCIENCE DIRECT

Bioorganic & Medicinal Chemistry 11 (2003) 3753–3760

BIOORGANIC & MEDICINAL CHEMISTRY

Three-Dimensional Molecular-Field Analyses of Octopaminergic Agonists for the Cockroach Neuronal Octopamine Receptor

Akinori Hirashima,[a,*] Masako Morimoto,[b] Eiichi Kuwano[a] and Morifusa Eto[c]

[a]*Department of Applied Genetics and Pest Management, Faculty of Agriculture, Graduate School, Kyushu University, Fukuoka 812-8581, Japan*

[b]*Department of Bioresource and Bioenvironmental Sciences, School of Agriculture, Kyushu University, 6-10-1 Hakozaki, Higashi-ku, Fukuoka 812-8581, Japan*

[c]*Professor Emeritus of Kyushu University, 7-32-2 Aoba, Higashi-ku, Fukuoka 813-0025, Japan*

Received 21 February 2002; revised 9 May 2003; accepted 12 May 2003

Abstract—The quantitative structure–activity relationship of a set of 40 octopaminergic agonists against receptor 2 in cockroach nervous tissue, was analyzed using molecular-field analysis (MFA). MFA on the study set of those compounds evaluated effectively the energy between a probe and a molecular model at a series of points defined by a rectangular grid. Contour surfaces for the molecular fields were presented and the results provided useful information in the characterization and differentiation of octopaminergic receptor.

Introduction

Octopamine [2-amino-1-(4-hydroxyphenyl)ethanol (OA)] which has been found to be present in high concentrations in various insect tissues, is the monohydroxyllic analogue of the vertebrate hormone noradrenalin. OA was first discovered in the salivary glands of octopus by Erspamer and Boretti in 1951. It has been found that OA is present in a high concentration in various invertebrate tissues.[1] This multifunctional and naturally occurring biogenic amine has been well studied and established as (1) a neurotransmitter, controlling the firefly light organ and endocrine gland activity in other insects; (2) a neurohormone, inducing mobilization of lipids and carbohydrates; (3) a neuromodulator, acting peripherally on different muscles, fat body, and sensory organs such as corpora cardiaca and the corpora allata, and (4) a centrally acting neuromodulator, influencing motor patterns, habituation, and even memory in various invertebrate species.[2,3] Three different receptor classes OAR1, OAR2A, and OAR2B had been distinguished from non-neuronal tissues.[4] The action of OAR2 is mediated through various receptor classes which is coupled to G-proteins and is specifically linked to an adenylate cyclase. Thus, the physiological actions of OAR2 have been shown to be associated with elevated levels of cAMP.[5] In the nervous system of locust *Locusta migratoria* L., a particular receptor class was characterized and established as a new class OAR3 by pharmacological investigations of the [^{3}H]OA binding site using various agonists and antagonists.[6–10]

Recently, much attention has been directed at the octopaminergic system as a valid target in the development of safer and selective pesticides.[11–13] Structure–activity studies of various types of OA agonists and antagonists were also reported using the nervous tissue of the migratory locust, *L. migratoria* L.[6–10] However, information on the structural requirements of these OA agonists and antagonists for high OA-receptor ligands is still limited. It is therefore of critical importance to provide information on the pharmacological properties

*Corresponding author. Tel.: +81-92-642-2856; fax: +81-92-642-2858; e-mail: ahirasim@agr.kyushu-u.ac.jp

0968-0896/03/$ - see front matter © 2003 Elsevier Ltd. All rights reserved.
doi:10.1016/S0968-0896(03)00313-4

of this OA receptor types and subtypes. Our interest in OA agonists was aroused by the results of quantitative structure–activity relationship (QSAR) studies using various physicochemical parameters as descriptors[14,15] and receptor surface model.[16] Furthermore, molecular modeling and conformational analysis were performed in Catalyst/Hypo to gain a better knowledge of the interactions between OA antagonists and OAR3 in order to understand the conformations required for binding activity.[17] A similar procedure was repeated using OA agonists.[18] However, binding activity is not enough for evaluating OA-agonist activity, since in binding assay it is difficult to say the difference of activities between OA agonists and antagonists. In drug discovery, it is common to have measured activity data for a set of compounds acting upon a particular protein but not to have knowledge of the three-dimensional structure of the protein active site. In the absence of such three-dimensional information, one can attempt to build a hypothetical model of the receptor site that can provide insight about receptor site characteristics. Such a model is known as a molecular-field analysis (MFA), which provides compact and quantitative descriptors which capture three-dimensional information about a putative receptor site. Thus, the current work is aimed to perform 3-D MFA on a set of OA agonists against thoracic nerve system of American cockroach *Periplaneta americana*, in which OA-agonist action is supposed to be due to cAMP elevation at OAR2.[12]

Results and Discussion

QSAR attempts to model the activity of a series of compounds using measured or computed properties of the compounds.[19–21] A set of 40 molecules, whose stimulatory activities of adenylate cyclase were tested using the radioimmunoassay (RIA) in the cockroach central nervous tissue, was selected as the target training set. The molecular structures and experimental biological activities are listed in Figure 1a and Table 1, respectively. V_{max} means the maximal response relative to OA and was expressed as the mean of four independent expreriments. Values of pK_a (log of the reciprocal of K_a) were used as OA-agonist activity index. K_a is the concentration of OA agonist necessary for half-maximal activation of adenylate cyclase. The K_a values were calculated from at least five concentrations ranging from 10^{-7} M to 10^{-3} M with a Macintosh personal computer system, using a sigmoidal curve-fitting program designed for log dose–probit activity analyses. 2-(4-Chloro-2-methylphenylimino)oxazolidine **30** showed the highest activity followed by 2-(2,6-diethylphenylimino)imidazolidine **39**, 2-(3-chlorobenzylamino)-2-oxazoline (CAO) **33**, OA **6**, and 1-(2,6-diethylphenyl)imidazolidine-2-thione **35** in study compounds. The compounds **35** and **39** showed the almost same V_{max} as OA, suggesting that only these compounds are full OA agonists and other compounds in Table 1 are partial OA agonists.

Figure 2 shows OA **6** and OA agonist arylethanolamine (AEA) **2** with the lowest activity embedded in an MFA generated from the OA-agonist data set. A rigid fit was performed to superimpose each structure so that it overlays the shape reference compound **30**. The field of the entire agonist data set is represented and only the structures of **6** and **2** are embedded within the contours. The blue surface represents a contour for those points that correspond to a probe to pK_a. The blue surface is embedded with the MeO group of the least active OA agonist **2**, and thus, decleasing OA activity. Figure 3 shows OA full agonist **39** and OA **6** embedded in an MFA generated from the OA-agonist data set. The ethyl group of **39** is superimposed with the aminoethanol side chain of **6**. The imidazoline ring of **39** sticks out of the surface and should be in a desirable position for its activity, since **39** has higher activity than OA. Similarly, Figure 4 shows another full OA agonist 3-(substituted phenyl)imidazolidine-2-thione (SPIT) **35** and OA embedded in an MFA generated from the OA-agonist data set. The ethyl group of **35** is superimposed with the aminoethanol side chain of **6**. The imidazoline ring of **35** sticks out of the surface and should be in a less desirable position for its activity compared to **39**, since **35** has lower activity than **39**.

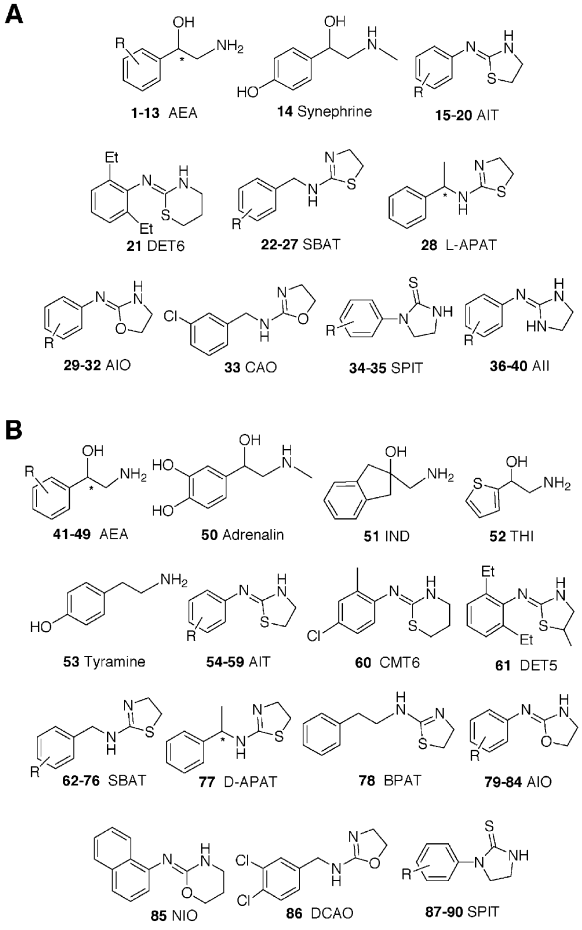

Figure 1. Structures of OA agonists used for regression analysis in study (A) and test (B) sets.

Table 1. Effect of OA agonists on the adenylate-cyclase activity in homogenates of American cockroach nerve cords[a] in study set

Compd		V_{max} (%)	K_a (μM)	pK_a		
No.	*R*			Observed	Calculated[b]	Deviation[c]
			AEA			
1	H (D)	34.2±1.1	215.24 (187.47–247.95)	3.67	3.71	−0.04
2	2-MeO	45.8±3.2	1506.37 (1218.42–1871.21)	2.82	2.74	0.08
3	4-Br	45.2±2.7	93.35 (84.46—103.29)	4.03	4.00	0.03
4	4-Cl	72.1±1.2	68.77 (62.72–75.51)	4.16	3.94	0.22
5	4-F	44.0±0.9	273.39 (252.31–296.76)	3.56	4.00	−0.44
6	4-OH (OA)	100.0±5.5	6.58 (6.01–7.19)	5.18	4.46	0.72
7	4-Me	52.0±1.4	77.95 (67.32–90.41)	4.11	4.16	−0.05
8	4-CF_3	31.8±1.5	99.82 (87.32–114.29)	4.00	3.78	0.22
9	2,4-Cl_2	31.0±3.6	192.30 (165.79–223.06)	3.72	3.88	−0.16
10	2,4-F_2	41.7±0.2	263.48 (235.45–295.11)	3.58	3.33	0.25
11	3,4-Cl_2	30.1±2.5	151.70 (128.67–180.74)	3.82	4.13	−0.31
12	3,4-$(OH)_2$	31.5±8.7	17.91 (14.86–21.63)	4.75	4.61	0.14
13	3,5-Cl_2	30.0±0.5	121.37 (98.43–149.89)	3.92	3.84	0.08
14	Synephrine	57.6±5.6	150.03 (125.77–179.70)	3.82	4.48	−0.66
			AIT			
15	2-Me,4-Br	41.1±1.1	23.62 (20.19–27.83)	4.63	4.70	−0.07
16	2-Me,4-Cl	36.7±3.8	3.09 (2.06–4.82)	5.51	5.29	0.22
17	2-Et,4-Br	31.2±3.0	16.14 (13.40–19.30)	4.79	4.88	−0.09
18	2,4-Me_2	55.0±3.9	13.65 (12.80–14.54)	4.86	4.85	0.01
19	2,6-Et_2	50.2±2.2	26.13 (25.04–27.26)	4.58	4.65	−0.07
20	2,4,6-Me_3	33.3±2.9	129.23 (121.12–137.77)	3.89	4.31	−0.42
21	DET6	39.8±3.6	158.92 (130.35–193.83)	3.80	3.94	−0.14
			SBAT			
22	2-Me	30.4±3.1	851.54 (573.55–1321.35)	3.07	3.24	−0.17
23	3-F	40.8±1.5	35.04 (29.43–41.65)	4.46	4.09	0.37
24	2,4-Cl_2	34.3±0.9	27.55 (18.99–38.81)	4.56	4.53	0.03
25	3,4-Cl_2	52.5±6.2	17.51 (14.45–21.29)	4.76	5.01	−0.25
26	3,5-Cl_2	45.7±4.6	16.25 (13.41–19.80)	4.79	4.71	0.08
27	3,5-F_2	33.2±4.9	84.90 (70.64–101.86)	4.07	4.11	−0.04
28	L-APAT	37.3±0.7	609.25 (552.91–672.55)	3.22	3.22	0
			AIO			
29	2-Me,4-Br	33.9±2.3	19.54 (16.00–24.38)	4.71	4.95	−0.24
30	2-Me,4-Cl	32.3±2.3	0.37 (0.26–0.50)	6.43	6.56	−0.13
31	2,6-Et_2	57.9±1.8	16.84 (13.92–20.19)	4.77	5.01	−0.24
32	2-Et,6-*i*Pr	42.5±0.8	13.16 (10.39–16.54)	4.88	4.66	0.22
33	CAO	40.0±1.1	5.07 (4.12–6.14)	5.29	5.39	−0.10
			SPIT			
34	2-Me,4-Cl	30.6±0.4	1.99 (1.61–2.47)	5.70	5.62	0.08
35	2,6-Et_2	104.0±1.6	8.08 (6.32–10.26)	5.09	5.05	0.04
			AII			
36	2-Et	33.0±14.8	3.84 (2.66–5.51)	5.42	5.31	0.11
37	2,6-Me_2	47.7±7.6	15.03 (11.38–19.92)	4.82	4.72	0.10
38	2-Me,6-Et	47.6±2.7	9.54 (7.48–12.10)	5.02	5.03	−0.01
39	2,6-Et_2	104.6±1.4	0.76 (0.49–1.13)	6.12	5.92	0.20
40	2,4,6-Me_3	59.1±10.2	8.40 (5.68–12.34)	5.08	4.73	0.35

[a]See the text for experimental details. The adenylate-cyclase activity of *P. americana* was measured according to Nathanson's procedure and the cAMP levels were measured by a RIA. Basal (control) and OA (100 μM)-stimulated (V_{max}) adenylate cyclase activities were 116.2±5.4 and 1,473.3±59.3 pmol cAMP/min/mg of protein, respectively. In parentheses, 95% confidence limits are shown. K_a and 95% confidence limit values were calculated with the Macintosh personal computer system using a sigmoidal curve-fitting program designed for log dose–probit activity analyses.

[b]Calculated by eq 1.

[c]Where predicted activity is overestimated, deviation is obtained by calculating predicted activity subtracted by experimental value and indicated by minus. Where predicted activity is underestimated, deviation is obtained by calculating experimental activity subtracted by predicted value.

In order to quantitatively understand the dependence of biological activities on MFA parameters of OA agonists, regression analysis was applied to representative 40 study compounds listed in Figure 1a and Table 1, leading to eq 1. The number of variables for eq 1 was 576 for CH_3 probe. Ten percent of all new significant columns of variables were automatically used as independent X variables in the generation of QSAR. In eq 1, the descriptors CH_3/x, CH_3/y, and CH_3/z are the energies between a methyl probe and the molecule at the rectangular points x, y, and z, respectively.

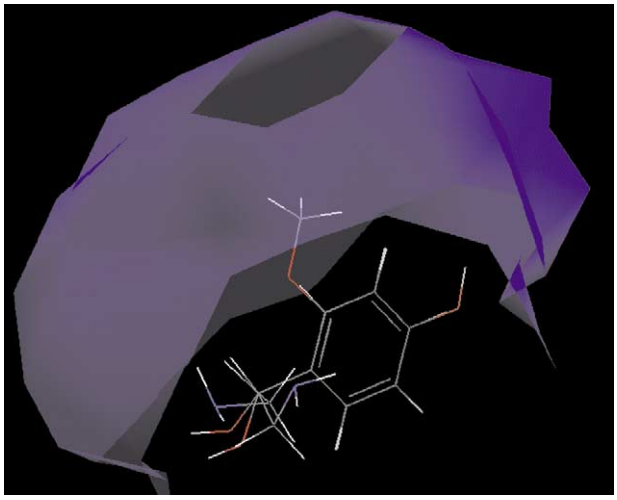

Figure 2. OA **6** and the least active OA agonist **2** embedded in an MFA generated from OA agonist data set.

$$\begin{aligned} \mathrm{p}K_a = {} & 5.9441 + 0.000216(H+/175)^2 - 0.000657 \\ & \times (H+/258)^2 + 0.000922 \\ & \times (H+/462)^2 - 0.000876 \\ & \times (CH_3/186)^2 - 0.001088 \\ & \times (CH_3/268-30)^2 - 0.000815 \\ & \times (CH_3/332)^2 - 0.000803 \\ & \times (CH_3/340-30)^2 + 0.000648 \\ & \times (CH_3/446-0.577188)^2 - 0.000257 \\ & \times (CH_3/301)^2 - 0.00083 \\ & \times (CH_3+/445)^2 - 0.000378 \\ & \times (CH_3+/447+6.64684)^2 - 0.000214 \\ & \times (CH_3-/177+2.70856)^2 + 0.000649 \\ & \times (HO-/265-30)^2 \end{aligned} \quad (1)$$

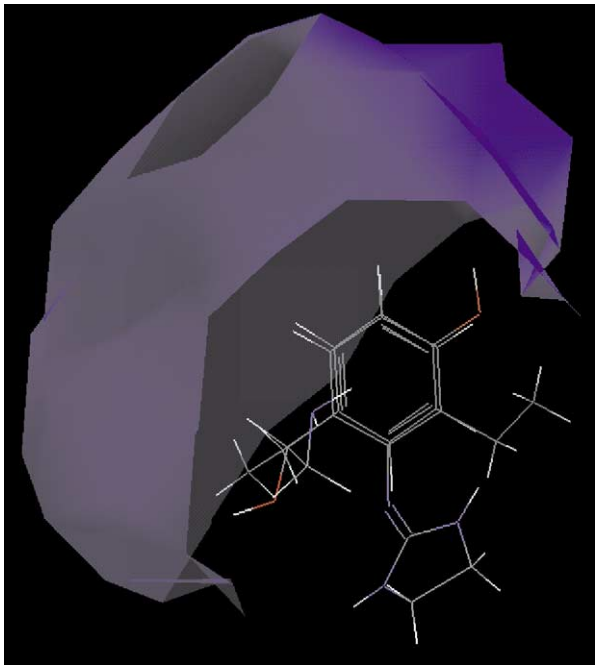

Figure 3. The OA agonist **39** with the highest activity and OA **6** embedded in an MFA generated from OA agonist data set.

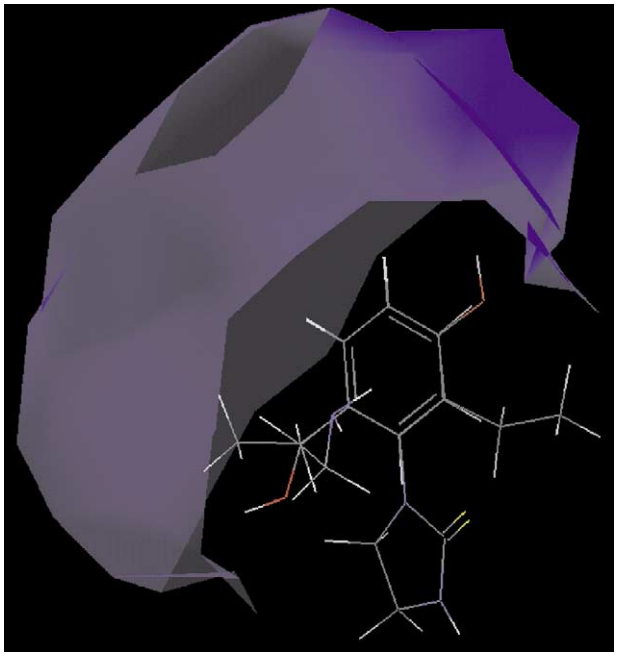

Figure 4. The OA agonist **35** and OA **6** embedded in an MFA generated from OA agonist data set.

where $n=40$, $r^2=0.906$, $CV{-}r^2=0.647$, PRESS $=8.855$, and $Bsr^2=0.868\pm0.171$. The term n means the number of data points; r-squared (r^2), the square of the correlation coefficient, which is used to describe the goodness of fit of the data of the study compounds to the QSAR model; cross-validated r^2 ($CV{-}r^2$), a squared correlation coefficient generated during a validation procedure using the equation: $CV{-}r^2=(\mathrm{SD}-\mathrm{PRESS})/\mathrm{SD}$; SD, the sum of squared deviations of the dependent variable values from their mean; predicted sum of squares (PRESS), the sum of overall compounds of the squared differences between the actual and the predicted values for the dependent variables. The PRESS value is computed during a validation procedure for the entire training set. The larger the PRESS value, the more reliable is the equation. A $CV{-}r^2$ is usually smaller than the overall r^2 for a QSAR equation. It is used as a diagnostic tool to evaluate the predictive power of an equation generated using the genetic partial least squares (G/PLS) method. Cross-validation is often used to determine how large a model (number of terms) can be used for a given data set. For instance, the number of

components retained in G/PLS can be selected to be that which gives the highest $CV{-}r^2$. Bootstrap r^2 (Bsr^2) is the average squared correlation coefficient calculated during the validation procedure.[22] A Bsr^2 is computed from the subset of variables used one-at-a-time for the validation procedure. It can be used more than one time in computing the r^2 statistic. Table 1 depicts structures of OA agonists, their experimental K_a values, calculated pK_a values using eq 1, and difference between observed and calculated pK_a values. In case predicted activity is overestimated, deviation is obtained by calculating predicted activity subtracted by experimental value and indicated by minus. In case predicted activity is underestimated, deviation is obtained by calculating experimental activity subtracted by predicted value. Residuals (observed versus calculated from Table 1) are plotted in Figure 5. The process of calculating an MFA does not treat the structures with low V_{max} values reasonably, possibly because it is misleading to evaluate K_a values of OA agonists when their V_{max} values are too low.

Some models were statistically significant and were used to correctly predict the activities of a set of test molecules ranging over three orders of magnitude (max. pK_a 6.43 and min. pK_a 2.82), indicating that these models could be useful tools to design active OA agonists. The predictive character of the QSARs was further assessed using test molecules, whose structures are shown in Figure 1b, outside of the training set. The best statistically significant eq 1 was applied to access these OA agonists. The predicted values of these molecules are listed in Table 2. Some OA agonists were active according to eq 1 in intracellular cAMP production. Residuals (observed versus calculated from Table 2) are plotted in Figure 6. These results may imply that the process of calculating an MFA treats these structures reasonably.

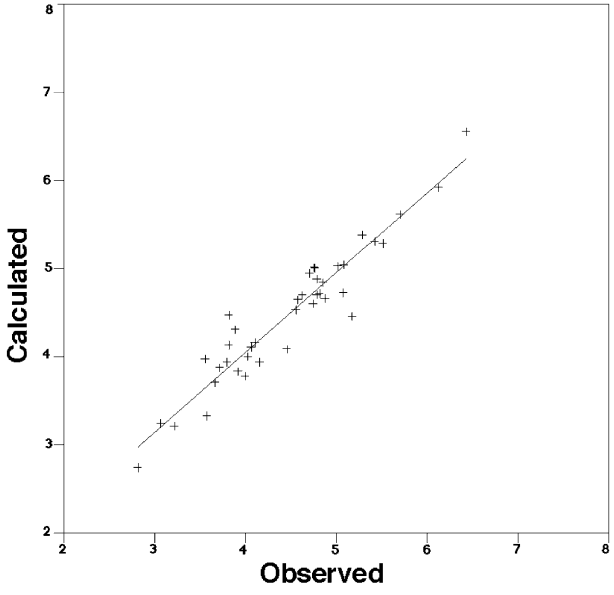

Figure 5. Correlation of observed pK_a values (horizontal) versus calculated pK_a values (vertical) from Table 1 using eq 1 in study set.

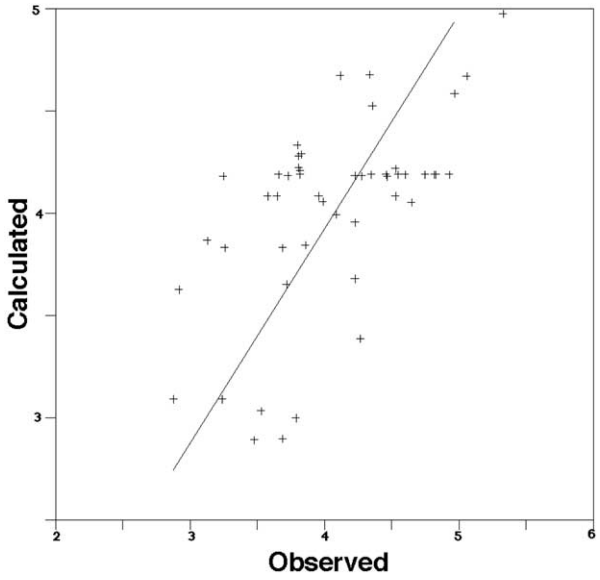

Figure 6. Correlation of observed pK_a values (horizontal) versus calculated pK_a values (vertical) from Table 2 using eq 1 in study set.

Conclusions

MFAs are quantitative and differ from pharmacophore models, which are qualitative, in that the former tries to capture essential information about the receptor, while the latter only captures information about the commonality of compounds that bind. MFAs tend to be geometrically overconstrained (and topologically neutral) since, in the absence of steric variation in a region, they assume the tightest steric surface which fits all training compounds. MFAs do not contain atoms, but try to directly represent the essential features of an active site by assuming complementarity between the shape and properties of the receptor site and the set of binding compounds. The MFA application uses 3-D surfaces that define the shape of the receptor site by enclosing the most active members (after appropriate alignment) of a series of compounds. The global minimum of the most active compound **30** in the study compounds (based on the value in the activity column) was made as the active conformer. When there is no information on the actual 'active conformation' of the ligands, MFA does not really describe the receptor; it describes a self-consistent field around the molecules that can explain activity. It really is just one of possibly many self-consistent models that fit the biological activity data.

OA is not likely to penetrate either the cuticle or the central nervous system of insects effectively, since it is fully ionized at physiological pH. Derivatization of the polar groups would be one possible solution to this problem in trying to develop potential pest-control agents. The above MFA studies show that full agonists with 2,6-diethyl substituents can be potential ligands to OA receptors. Phenyl ring substitution requirements for partial OA agonists differ substantially from each other and other various types of OA agonists could be potent, although the type of

Table 2. Effect of OA agonists on the adenylate–cyclase activity in homogenates of American cockroach nerve cords[a] in test set

Compd		V_{max} (%)	K_a (μM)	pK_a		
No.	R			Observed	Calculated[b]	Deviation[c]
			AEA			
41	H (L)	11.1±3.4	262.57 (193.61–344.80)	3.58	4.09	−0.51
42	3–Br	13.4±0.9	154.00 (103.75–232.52)	3.81	4.22	−0.41
43	3–Cl	19.0±0.6	157.63 (128.21–193.68)	3.80	4.34	−0.54
44	3–Me	22.5±2.0	740.43 (625.83–880.08)	3.13	3.87	−0.74
45	4–NO_2	33.9±0	298.36 (280.53–317.65)	3.53	3.03	0.50
46	2,3–Cl_2	15.6±0.9	137.24 (82.00–212.16)	3.86	3.85	0.01
47	2,4–Me_2	11.6±0.9	217.75 (109.38–449.32)	3.66	4.19	−0.53
48	2,6–F_2	21.2±1.3	1515.61 (1147.91–2060.88)	2.92	3.63	−0.71
49	2,6–$(MeO)_2$	16.6±0.4	555.13 (334.87–917.15)	3.26	3.83	−0.57
50	Adrenalin	21.7±3.5	43.85 (33.95–56.73)	4.36	4.53	−0.17
51	IND	13.8±0.8	581.64 (358.11–1025.27)	3.24	3.09	0.15
52	THI	18.5±1.5	1328.80 (849.64–2218.85)	2.88	3.09	−0.21
53	Tyramine	22.4±5.6	24.88 (19.65–31.28)	4.60	4.19	0.41
			AIT			
54	2–Et	12.3±2.5	33.98 (30.91–37.36)	4.47	4.18	0.29
55	2–Br,4–Me	25.0±2.5	148.39 (136.27–161.37)	3.83	4.29	−0.46
56	2,5–$(MeO)_2$	18.5±2.2	565.29 (528.81–603.49)	3.25	4.18	−0.93
57	2–Et,6–*i*Pr	24.4±3.5	75.64 (71.80–79.70)	4.12	4.68	−0.56
58	3,5–Cl_2	7.7±0.7	153.19 (24.59–1066.62)	3.81	4.28	−0.47
59	2,6–Me_2,4–Br	19.3±2.3	52.74 (36.15–81.42)	4.28	4.18	0.10
60	CMT6	16.0±0.8	205.01 (144.37–280.93)	3.69	2.90	0.79
61	DET5	13.3±1.2	151.32 (119.24–191.64)	3.82	4.21	−0.39
			SBAT			
62	H	20.9±1.0	29.51 (17.86–56.69)	4.53	4.22	0.31
63	2–Cl	24.3±1.5	192.02 (105.91–315.60)	3.72	3.65	0.07
64	2–F	29.1±0.6	162.88 (122.07–230.02)	3.79	3.00	0.79
65	2–CF_3	23.2±0.4	17.66 (13.12–23.50)	4.75	4.19	0.56
66	3–Me	26.1±0.7	11.66 (7.10–18.33)	4.93	4.19	0.74
67	4–Me	25.5±1.8	53.85 (36.19–79.85)	4.27	3.39	0.88
68	4–MeO	28.5±0.6	4.65 (3.06–6.99)	5.33	4.98	0.35
69	2–Cl,4–F	18.6±2.1	59.24 (39.17–88.14)	4.23	3.96	0.27
70	2–F,4–Cl	29.2±1.9	22.63 (18.86–27.11)	4.65	4.06	0.59
71	2,4–F_2	23.9±4.2	202.31 (160.47–257.62)	3.69	3.83	−0.14
72	2,5–F_2	26.9±6.0	45.42 (35.91–56.86)	4.34	4.68	−0.34
73	2,6–F_2	8.9±1.5	28.49 (9.85–69.87)	4.55	4.19	0.36
74	2,6–$(MeO)_2$	8.1±0.6	59.09 (23.25–141.57)	4.23	4.19	0.04
75	3–Cl,4–F	12.3±0.7	10.74 (3.93–22.72)	4.97	4.59	0.38
76	3,4–F_2	19.3±2.9	80.36 (59.83–111.14)	4.09	3.99	0.10
77	D–APAT	16.0±1.2	328.60 (252.17–4321.21)	3.48	2.89	0.59
78	BPAT	22.7±0.6	185.65 (27.84–861.26)	3.73	4.19	−0.46
			AIO			
79	4–Et	27.0±3.4	109.07 (86.463–137.02)	3.96	4.09	−0.13
80	2–MeO,5–Me	15.7±1.1	28.38 (19.78–40.31)	4.55	4.19	0.36
81	2–Me,6–*i*Pr	15.6±0.4	44.68 (19.03–92.57)	4.35	4.19	0.16
82	2,6–*i*Pr_2	13.9±1.4	152.20 (100.57–219.87)	3.82	4.19	−0.37
83	2,3,4–Cl_3	30.0±0.2	102.03 (74.15–131.27)	3.99	4.06	−0.07
84	2,3,4,5–Cl_4	27.0±2.0	29.68 (24.45–36.23)	4.53	4.09	0.44
85	NIO	11.6±0.2	8.76 (5.95–12.49)	5.06	4.67	0.39
86	DCAO	28.6±0.7	14.71 (11.47–18.77)	4.83	4.19	0.64
			SPIT			
87	2,4–Cl_2	17.8±0.1	226.03 (151.51–330.84)	3.65	4.09	−0.44
88	2,4–Me_2	10.5±0.5	34.64 (18.50–59.33)	4.46	4.19	0.27
89	2–MeO,5–Me	15.4±2.1	15.22 (8.29–23.80)	4.82	4.19	0.63
90	2,6–*i*Pr_2	23.8±0.3	59.49 (46.85–75.42)	4.23	3.68	0.55

[a]See the text for experimental details. The adenylate-cyclase activity of *P. americana* was measured according to Nathanson's procedure and the cAMP levels were measured by a RIA. Basal (control) and OA (100 μM)-stimulated (V_{max}) adenylate cyclase activities were 116.2±5.4 and 1,473.3±59.3 pmol cAMP/min/mg of protein, respectively. In parentheses, 95% confidence limits are shown. K_a and 95% confidence limit values were calculated with the Macintosh personal computer system using a sigmoidal curve-fitting program designed for log dose–probit activity analyses.

[b]Calculated by eq 1.

[c]In case predicted activity is overestimated, deviation is obtained by calculating predicted activity subtracted by experimental value and indicated by minus. In case predicted activity is underestimated, deviation is obtained by calculating experimental activity subtracted by predicted value.

compounds tested here is still limited to draw any conclusions. These derivatives could provide useful information in the characterization and differentiation of OA receptor. They may help to point the way towards developing extremely potent and relatively specific OA ligands, leading to potential insecticides, although further research on the comparison of the 3-D QSAR from agonists is necessary. In order to optimize

the activities of these compounds as OA ligands, more detailed experiments are in progress.

Experimental

Synthesis of OA agonists

AEAs **1** and **41** were obtained by reducing mandelic acid via its ester and amide with lithium aluminum hydride (LAH)[23] and other AEAs **3–13**, **42–49**, 2-aminomethyl-2-indanol (IND) **51**, and 2-amino-1-(2-thiazoyl)ethanol (THI) **52** were synthesized from trimethylsilyl cyanide and the corresponding aldehydes in the presence of catalytic amount of anhydrous zinc iodide, followed by reduction with LAH.[24] 2-(Arylimino)thiazolidines (AITs) **15–20**, **54–59**, 2-(2,6-diethylphenylimino)thiazine (DET6) **21**, 2-(substituted benzylamino)-2-thiazolines (SBATs) **22–27**, **62–76**, 2-(α-phenylethylamino)-2-thiazolines (APATs) **28**, **77**, 2-(4-chloro-2-methylphenylimino)thiazine (CMT6) **60**, 2-(2,6-diethylphenylimino)-5-methylthiazolidine (DET5) **61**, and 2-(β-phenylethylamino)-2-thiazoline (BPAT) **78** were synthesized by cyclization of the corresponding thioureas with concd hydrogen chloride.[25] 2-(Arylimino)oxazolidines (AIOs) **29–32**, **79–84**, 2-(1-naphthylimino)oxazolidine (NIO) **85,** CAO **33**, and 2-(3,5-dichlorobenzylamino)-2-oxazoline (DCAO) **86** were obtained by cyclodesulfurizing the corresponding thioureas with yellow mercuric oxide.[26] SPITs **34**, **35**, and **87–90** were synthesized by the cyclization of monoethanolamine hydrogen sulfate with the corresponding arylisothiocyanates in the presence of sodium hydroxide as described in the previous report.[27] 2-(Arylimino)imidazolidine (AII) **36–40** were prepared according to a reported method by refluxing the corresponding anilines and 1-acetyl-2-imidazolidone in phosphoryl chloride followed by hydrolysis.[28] The structures of the compounds were confirmed by ^{1}H, ^{13}C NMR measured with a JEOL JNM-EX400 spectrometer at 400 MHz, tetramethyl silane (TMS) being used as an internal standard for ^{1}H NMR, and elemental analytical data.

Chemicals

DL-Noradrenalin **12** hydrochloride was purchased from Janssen Chimica (Beerse, Belgium); GTP and DL-synephrine **14** were from Sigma Chemical Co. (St. Louis, USA); ATP disodium salt was from Kohjin Co. (Tokyo, Japan); LAH was from Chemetall GmbH (Frankfurt, Germany); DL-adrenalin **50** hydrochloride was from Tokyo Chem. Ind. Co. Ltd. (Tokyo, Japan); OA, theophylline (1,3-dimethylxanthine), tyramine **53**, and ethylene glycol bis(β-aminoethyl ether)-*N*,*N*,*N*′,*N*′-tetraacetic acid (EGTA) were from Nacalai Tesque (Kyoto, Japan).

Biological assay

Insect culture. Males and females of *P. americana* were used indiscriminately, as their nervous systems exhibited no gross structural or neurochemical differences. The insects were reared under crowded conditions in this laboratory at 28 °C with a photoperiod of 12 h light/12 h dark and at a relative humidity of 65–70% for more than 10 years; they were provided with an artificial mouse diet (Oriental Yeast Co., Chiba, Japan) and water ad libitum.

Radiochemical. The cAMP RIA kit (cord RPA 509) was purchased from Amersham International (Buckinghamshire, UK).

Adenylate-cyclase assay. The adenylate-cyclase assay was conducted on adult American cockroaches (*P. americana*) as shown in previous report.[12,25–27] Thoracic nerve cords of *P. americana* were homogenized (15 mg/mL) in a 6-mM Tris–maleate buffer (pH 7.4) by using a chilled microtube homogenizer (S-203, Ikeda Sci., Tokyo, Japan) as shown in previous report. The homogenate was diluted (1 mg/mL) in 6 mM Tris–maleate, and then centrifuged at 120,000*g* and 4 °C for 20 min. The supernatant was discarded, the pellet being resuspended by homogenizing (1 mg/mL) in the buffer, and again centrifuged at 120,000*g* and 4 °C for 20 min. The resulting pellet (P2) resuspended in the buffer was equivalent to the starting amount (15 mg/mL). The adenylate-cyclase activity was measured according to Nathanson's procedure under optimal conditions[12,25–27] in a test tube containing 200 μL of 120 mM Tris–maleate (pH 7.4, including 15 mM theophylline, 12 mM $MgCl_2$, and 0.75 mM EGTA), 60 μL of the P2 fraction, and 30 μL of each synthesized compound solution in polyethylene glycol. An appropriate solvent control was run in parallel. The enzyme reaction (5 min at 30 °C) was initiated by adding 10 μL of a mixture of 3 mM GTP and 60 mM ATP, stopped by heating at 90 °C for 2 min and then centrifuged at 1000*g* for 15 min to remove the insoluble material. The cAMP level in the supernatant was measured by RIA.[12,25–27] Protein concentration was determined by the Lowry method,[29] using bovine serum albumin (Sigma, St. Louis, USA) as the standard. Enzyme activity in each assay was corrected using OA as a reference. The V_{max} values (mostly at 0.1 mM) was calculated relative to OA (100%) and control (0%).

Computational details

Molecular alignment. All experiments were conducted with Cerius2 3.8 QSAR environment from Accelrys (Burlington, MA, USA) on a Silicon Graphics O2, runnning under the IRIX 6.5 operating system. Multiple conformations of each molecule were generated using the Boltzmann Jump as a conformational search method. The upper limit of the number of conformations per molecule was 150. Each conformer was subjected to an energy minimization procedure to generate the lowest energy conformation for each structure. Alignment of structures through pair-wise superpositioning placed all structures in the study compounds in the same frame of reference as the shape reference compound, which was selected as a conformer of the most active OA agonist **30**. The method used for performing the alignment was maximum common subgroup (MCSG). This method looks at molecules as points and lines, and uses the techniques of graph theory to identify patterns. It finds the largest subset of atoms in the shape reference compound that is shared by all the structures in the study table and uses this subset for

alignment. A rigid fit of atom pairings was performed to superimpose each structure so that it overlays the shape reference compound. The Naturally ocurring S form was used for catecholamines noradrenalin **12** and adrenalin **50**, and R form was used for monophenolamines OA **6** and synephrine **14** in calculating the model.

MFA. MFA models are predictive and sufficiently reliable to guide the chemist in the design of novel compounds. These descriptors are used for predictive QSAR models. This approach is effective for the analysis of data sets where activity information is available but the structure of the receptor site is unknown. MFA attempts to postulate and represent the essential features of a receptor site from the aligned common features of the molecules that bind to it. This method generates multiple models that can be checked easily for validity. The MFA formalism calculates probe interaction energies on a rectangular grid around a bundle of active molecules. The surface is generated from a 'Shape Field'. The atomic coordinates of the contributing models are used to compute field values on each point of a 3-D grid. Grid size was adjusted to default 2.00 Å, since decreasing grid size to 1.00 Å did not help to improve the model. MFA evaluates the energy between a probe ($H+$, CH_3, CH_3+, CH_3-, $OH-$, and Donor/Acceptor) and a molecular model at a series of points defined by a rectangular grid. Fields of molecules are represented using grids in MFA and each energy associated with an MFA grid point can serve as input for the calculation of a QSAR. These energies were added to the study table to form new columns headed according to the probe type. The charges of the target molecules and probes have not been calculated.

G/PLS. Due to the large number of points used as independent variables, G/PLS was used to derive the QSAR models. G/PLS, a variation of genetic function approximation (GFA), can be run as an alternative to the standard GFA algorithm. G/PLS is derived from the best features of two methods: GFA and partial least squares (PLS). Both GFA and PLS have been shown to be valuable analysis tools in cases where the data set has more descriptors than samples. In PLS, variables might be overlooked during interpretation or in designing the next experiment even though cumulatively they are very important. This phenomenon is known as 'loading spread'. In GFA, equation models have a randomly chosen proper subset of the independent variables. As a result of multiple linear regression on each model, the best ones become the next generation and two of them produce an offspring. This was repeated 10,000 (default 5000) times. For other settings, all defaults were used. Loading spread does not occur because at most one of a set of co-linear variables is retained in each model. G/PLS combines the best features of GFA and PLS.[22] Each generation has PLS applied to it instead of multiple linear regression, and so each model can have more terms in it without danger of over-fitting. G/PLS retains the ease of interpretation of GFA by back-transforming the PLS components to the original variables.

Acknowledgements

This work was supported in part by a Grant-in-Aid for Scientific Research from the Ministry of Education, Science, and Culture of Japan.

References and Notes

1. Axelrod, J.; Saavedra, J. M. *Nature* **1977**, *265*, 501.
2. Evans, P. D. In *Comparative Molecular Neurobiology*; Heller, S. R., Ed.; Birkhäuser: Basel, 1993, p 287.
3. Evans, P. D. In *Comprehensive Insect Physiology Biochemistry Pharmacology*; Kerkut, G. A., Gilbert, G., Eds.; Pergamon: Oxford, 1985; Vol. 11, p 499.
4. Evans, P. D. *J. Physiol.* **1981**, *318*, 99.
5. Nathanson, J. A. *Mol. Pharmacol.* **1985**, *28*, 254.
6. Roeder, T.; Nathanson, J. A. *Neurochem. Res.* **1993**, *18*, 921.
7. Roeder, T.; Gewecke, M. *Biochem. Pharmol.* **1990**, *39*, 1793.
8. Roeder, T. *Life Sci* **1992**, *50*, 21.
9. Roeder, T. *Br J.Pharmacol.* **1995**, *114*, 210.
10. Roeder, T. *T.Eur J.Pharmacol.* **1990**, *191*, 221.
11. Jennings, K. R.; Kuhn, D. G.; Kukel, C. F.; Trotto, S. H.; Whiteney, W. K. *Pestic. Biochem. Physiol.* **1988**, *30*, 190.
12. Hirashima, A.; Yoshii, Y.; Eto, M. *Pestic. Biochem. Physiol.* **1992**, *44*, 101.
13. Ismail, S. M. M.; Baines, R. A.; Downer, R. G. H.; Dekeyser, M. A. *Pestic. Sci.* **1996**, *46*, 163.
14. Hirashima, A.; Shinkai, K.; Pan, C.; Kuwano, E.; Taniguchi, E.; Eto, M. *Pestic. Sci.* **1999**, *55*, 119.
15. Pan, C.; Hirashima, A.; Tomita, J.; Kuwano, E.; Taniguchi, E.; Eto, M. *Internet J. Sci. Biol. Chem.* **1997**, *1* (http://www.netsci-journal.com/97v1/97013/index.htm).
16. Hirashima, A.; Pan, C.; Tomita, J.; Kuwano, E.; Taniguchi, E.; Eto, M. *Bioorg. Med. Chem.* **1998**, *6*, 903.
17. Pan, C.; Hirashima, A.; Kuwano, E.; Eto, M. *J. Mol. Model.* **1997**, *3*, 455.
18. Hirashima, A.; Pan, C.; Kuwano, E.; Taniguchi, E.; Eto, M. *Bioorg. Med. Chem.* **1999**, *7*, 1437.
19. Hansch, C.; Leo, A.; Hoeckman, D. H., Eds., In *Exploring QSAR: Fundamentals and Applications in Chemistry and Biology*; American Chemical Society: Washington, DC, 1995; Vol. 1.
20. Hansch, C.; Fujita, T. *J. Am. Chem. Soc.* **1964**, *86*, 1616.
21. Golender, V. E.; Vorpagel, E. R. In *3-D-QSAR in Drug Design: Theory, Methods, and Applications*; Kubinyi, H., Ed.; ESCOM Science: Leiden, The Netherlands, 1993; p 137
22. *Cerius2 Tutorial*; Accelrys Inc. Burlington, MA, USA (http://www.accelrys.com/cerius2).
23. Wu, S.-Y.; Hirashima, A.; Takeya, R.; Eto, M. *Agric. Biol. Chem.* **1989**, *53*, 165.
24. Hirashima, A.; Yoshii, Y.; Kumamoto, K.; Oyama, K.; Eto, M. *J. Pestic. Sci.* **1990**, *15*, 539.
25. Hirashima, A.; Tarui, H.; Eto, M. *Biosci. Biochem. Biotech.* **1994**, *58*, 1206.
26. Hirashima, A.; Pan, C.; Katafuchi, Y.; Taniguchi, E.; Eto, M. *J. Pestic. Sci.* **1996**, *21*, 419.
27. Hirashima, A.; Shinkai, K.; Kuwano, E.; Taniguchi, E.; Eto, M. *Biosci. Biotech. Biochem.* **1998**, *62*, 1179.
28. Nathanson, J. A.; Kaugars, G. *J. Med. Chem.* **1989**, *32*, 1795.
29. Lowry, O. H.; Rosebrough, N. J.; Farr, A. L.; Randall, R. J. *J. Biol. Chem.* **1951**, *193*, 265.